CAVE DETECTION USING OBLIQUE THERMAL IMAGING. T. N. Titus[1], J. J. Wynne[2,3], M. D. Jhabvala[4], G. E. Cushing[1], P. Shu[4], N. A. Cabrol[3]; [1]U.S. Geological Survey, Astrogeology Science Center, 2255 N. Gemini Dr., Flagstaff, AZ 86001 (ttitus@usgs.gov); [2]Colorado Plateau Research Station, Northern Arizona University, Flagstaff, Arizona 86011; [3]The SETI Institute, Carl Sagan Center, Mountain View, CA 94043; [4]NASA Goddard Space Flight Center, Greenbelt, Maryland 20771.

Introduction: Caves provide access to the subsurface without the need for drilling and provide a wealth of interdisciplinary science – ranging from the geological and hydrological processes that formed the caves to the study of cave micro-climates and the biodiversity that exists within these unique environments.

On other planets and moons, where surface conditions are currently inhospitable to life as we know it – caves may either provide shelter for extant life or preserve evidence of past life [e.g., 1]. Caves and cave-like structures are also of interest because they may ultimately provide a lower-cost option for sheltering human explorers or provide access to much needed resources, such as water ice.

Unfortunately, caves may be elusive to detect. On Earth, caves are often discovered by accident. Typical methods for detecting caves include ridge-walking, early morning scanning for plumes or steam [e.g., 2,3], and thermal imaging [4,5]. Here we discuss the latter of these techniques.

Thermal imaging techniques have shown promise and some limited successes in the search for (or the confirmation of) possible caves and cave-like features on other planets.

Study Site Location: The site for this study was the Pisgah lava flow, near Ludlow, CA. This site has been used as a Mars analog, including the Viking and Pathfinder landing sites [6]. The Pisgah lava flow consists of Quaternary basaltic lava and a cinder cone superimposed on alluvial deposits and the lacustrine sediments of Lavic Lake playa [7]. The Pisgah flow erupted in three phases and consists of both `a`a and pahoehoe which vary in thickness from 1-5 meters [8]. The flows have multiple lava tubes, trenches, and alcoves, which makes this an ideal site to test the use of thermal imaging for cave and cave-like feature detection. The cinder cone provides an elevated platform for oblique viewing of the flow.

Data Collected:

Thermal Images: Using a QWIP (Quantum Well Photodetector) camera, we collected thermal imagery of the Pisgah lava flows (Fig. 1). Imagery was collected from a single station (2 different viewing azimuths), approximately half-way up the cinder cone, every 5 minutes over ~24 hrs, 23-25 March 2010 (244 images captured). Within one field of view was a trench containing several alcoves. One of these alcoves is visible within the thermal images (see Fig. 1- the red region in the center of the image). The other field of view acquired (not shown here) had a lateral entrance to a cave located in the centered in the images.

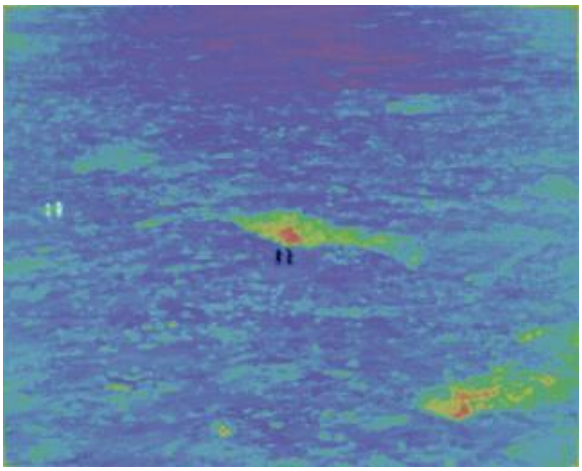

Figure 1: Pre-dawn Image of Co-Is Wynne and Titus identifying sensor locations. The intensity of the image is determined by differencing two TIR images acquired 5 minutes apart. The color is the pre-dawn temperature of the surface. In this figure, Titus and Wynne mark the positions of two sensor locations.

Surface Temperatures: For both fields of view, in-situ temperature sensors were used to simultaneously acquire surface temperatures within the thermal infrared images – thus connecting temperature data acquired from ground sensors to the thermal signature "seen" from thermal remote sensing. Figure 2 shows one of the in-situ sensor locations. An external temperature probe was inserted into the top 25 mm of the soil or rock. Internal temperature sensors were typically placed in locations such as cairns. A temperature and relative humidity sensor was placed on a 4 foot rebar rod approximately 1 meter above ground. The sensor was wrapped in aluminum foil to minimize impact from direct solar insolation. Figure 1 illustrates how we co-registered the sensor locations to image pixels. The sensors are located between the 2 people at their feet.

Analysis:

Thermal Conductivity: Figure 3 shows the results of comparing 1 in-situ data set to the DN values of the corresponding image pixel. A direct comparison between image DN and surface temperature shows a time lag between remotely sensed temperature (DN) and "ground truth." This is a direct consequence of the

thermal probe being a finite, non-zero length. However, the thermal conductivity can be estimated from the time-lag, and the "true" surface temperatures can be calculated by correcting the measured temperatures for time-lag and attenuation as described by the thermal diffusion equation.

Figure 2: Sensor arrangement to measure rock surface, cairn, and air temperatures.

Principle Component Analysis (PCA): PCA is a multivariate technique that can be used to reduce the dimensionality of a data set. PCA analysis identifies the parameters with the largest variations. For this analysis, we used each pixel DN value acquired throughout the 24-hour period as that pixel's coordinate within a 288-parameter space. Figure 4 shows the image constructed from the first eigenvector and a scatter plot of each pixel within the first 2 eigenvectors. A cluster of pixels are highlighted in red in both the image and the scatter plot – identifying the location of the alcove within the trench wall.

Conclusions: Oblique thermal imaging is a valid technique for detecting caves and cave-like structures. The thermal detectability of caves is best accomplished with multiple images acquired at the hottest time of day (early afternoon) and the coldest time of day (dawn). High thermal inertia material (e.g., rocks) exhibit similar diurnal thermal behavior and can only be reliably differentiated from caves in a single time of day image.

References: [1] Boston, P. et al. (1992) *Icarus, 95,* 300. [2] Faust B. (1947) *Natl. Speleol. Soc. Bull. 9,* 52–54. [3] Halliday W.R. (1954) *Natl. Speleol. Soc. Bull. 16,* 3–28. [4] Rinker A. B. and Author C. D. (1997) *JGR, 90,* 1151–1154. [5] Wynne J. J. and Author C. D. (1997) *JGR, 90,* 1151–1154. [6] Guiness, E.A. et al. (1997) *JGR, 102,* 28,687–28,703. [7] Dibblee, T.W. (1966) *USGS Map I-472.* [8] Gaddis L. R. (1994) *GRL, 21,* 1803–1806.

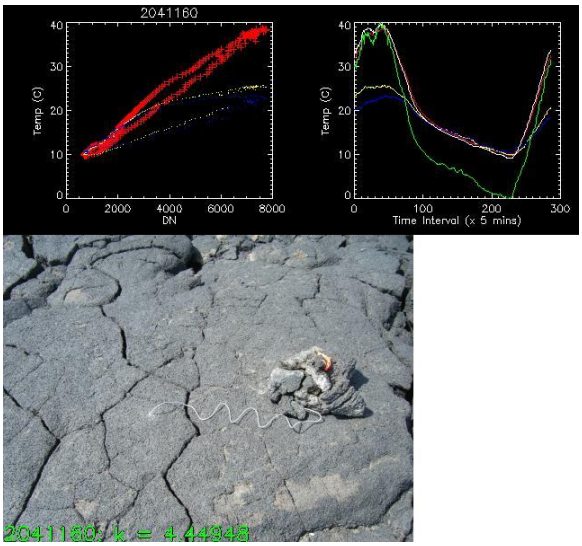

Figure 3: Sensor Number 2041160 - Red is the uncorrected surface temperature. Yellow is the cairn temperature and blue is the air temperature at 1 meter above ground. The same air temperature is used for all locations. The green is the scaled DN level from the thermal infrared camera. The white line is the surface temperature from the in-situ sensor when corrected for thermal inertia effects due to the temperature probe being a finite, non-zero length.

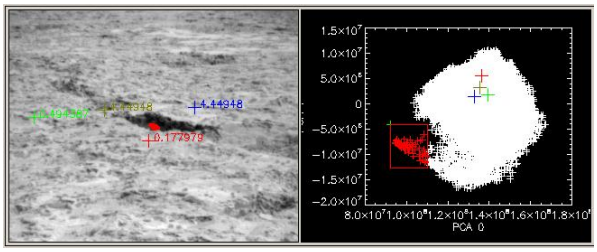

Figure 4: PCA Analysis of image time lapse cube. (Left) Image of the lava flow with a trench and cave-like alcove (red pixels). The plus signs indicate locations of temperature sensors. (Right) A PCA plot. Plus signs indicate locations of the pixels where temperature sensors were located within PCA space. The red highlighted box corresponds to the red pixels in the left panel.